

Electronic and thermoelectric properties of alkali metal-based perovskites $CsYbF_3$ and $RbYbF_3$

Q Mahmood, N A Noor, T Ghrib, Nessrin A Kattan, Asif Mahmood, Shahid M Ramay

Citation: Chin. Phys. B . 2020, 29(11): 117305 . **doi:** 10.1088/1674-1056/ab9de3
Journal homepage: http://cpb.iphy.ac.cn; http://iopscience.iop.org/cpb

What follows is a list of articles you may be interested in

Ab initio study of H/O trapping and clustering on U/Al interface

Wenhong Ouyang(欧阳文泓), Wensheng Lai(赖文生), Zhengjun Zhang(张政军)
Chin. Phys. B . 2018, 27(9): 097303 . **doi:** 10.1088/1674-1056/27/9/097303

Adsorptions of metal adatoms on graphene-like BC_3 and their rich electronic properties: A first-principles study

Pengfei Sui(隋鹏飞), Jiaqi Dai(戴佳琦), Yinchang Zhao(赵银昌), Zhenhong Dai(戴振宏)
Chin. Phys. B . 2018, 27(9): 097311 . **doi:** 10.1088/1674-1056/27/9/097311

Quantum spin Hall insulators in chemically functionalized As (110) and Sb (110) films

Xiahong Wang(王夏烘), Ping Li(李平), Zhao Ran(冉召), Weidong Luo(罗卫东)
Chin. Phys. B . 2018, 27(8): 087305 . **doi:** 10.1088/1674-1056/27/8/087305

Effect of metal catalyst on the mechanism of hydrogen spillover in three-dimensional covalent-organic frameworks

Xiu-Ying Liu(刘秀英), Jing-Xin Yu(于景新), Xiao-Dong Li(李晓东), Gui-Cheng Liu(刘桂成), Xiao-Feng Li(李晓凤), Joong-Kee Lee
Chin. Phys. B . 2017, 26(2): 027302 . **doi:** 10.1088/1674-1056/26/2/027302

First-principles study of structural, electronic, and optical properties of cubic $InAs_xN_yP_{1-x-y}$ triangular quaternary alloys

I Hattabi, A Abdiche, F Soyalp, R Moussa, R Riane, K Hadji, S Bin-Omran, R Khenata
Chin. Phys. B . 2017, 26(1): 017303 . **doi:** 10.1088/1674-1056/26/1/017303

Electronic and thermoelectric properties of alkali metal-based perovskites $CsYbF_3$ and $RbYbF_3$*

Q Mahmood[1,2,†], N A Noor[3], T Ghrib[1,2], Nessrin A Kattan[4], Asif Mahmood[5,‡], and Shahid M Ramay[6]

[1] *Basic and Applied Scientific Research Center, Imam Abdulrahman Bin Faisal University, P. O. Box* 1982, 31441, *Dammam, Saudi Arabia*
[2] *Department of Physics, College of Science, Imam Abdulrahman Bin Faisal University, P. O. Box* 1982, 31441, *Dammam, Saudi Arabia*
[3] *Department of Physics, Riphah International University, Lahore, Pakistan*
[4] *Department of Physics, Faculty of Science, Taibah University, Medina, Saudi Arabia*
[5] *Chemical Engineering Department, College of Engineering, King Saud University, Riyadh, Saudi Arabia*
[6] *Physics and Astronomy Department, College of Science, King Saud University Riyadh, Riyadh, Saudi Arabia*

(Received 3 March 2020; revised manuscript received 4 May 2020; accepted manuscript online 18 June 2020)

The electronic and thermoelectric properties of alkali metal-based fluorides $CsYbF_3$ and $RbYbF_3$ are studied by using Wien2k and BoltzTraP codes. The structural and thermodynamic stability of these materials are confirmed by tolerance factor (0.94 and 0.99 for $RbYbF_3$ and $CsYbF_3$) and negative formation energy. The optimized lattice constants and bulk moduli are consistent with the results reported in the literature. The reported band gap for $RbYbF_3$ is 0.86 eV which decreases to 0.83 eV by the replacement of Cs with Rb. The electrical and thermal conductivities along with Seebeck coefficients decrease with temperature rising from 0 K to 800 K. The large values of thermoelectric parameters for positive chemical potentials show that the character is dominated by electrons. The studied materials have figures of merit 0.82 and 0.81 at room temperature respectively, for $RbYbF_3$ and $CsYbF_3$ and increase with temperature rising. Therefore, the materials under study may have potential application values in thermoelectric generators and refrigerators.

Keywords: density functional theory, thermodynamic stability, electrical conductivity, figure of merit

PACS: 73.50.Lw **DOI:** 10.1088/1674-1056/ab9de3

1. Introduction

Investigation of physical properties of a material plays a key role in determining its technological importance. Although a huge variety of technically important materials have been developed already, perovskite represents a well-known class of material with impressive physical properties and technological importance. The importance and significance of these materials have been proved due to their good magnetic, optical, electrical as well as piezoelectric response to external motivation.[1–3] Moreover, ferroelectric performance, charge, and thermo-electric power generation are the prominent features of these materials. The applications of perovskites in sensors, substrates, filed effect transistors (FETs), fuel cell electrodes, and optoelectronic appliances with adaptable nature have been reported.[4–9] The halide-based perovskites have gained attention of researchers to probe their structural, magnetic, electronic, and optical properties due to their potential applications in device fabrication.[10] Fluoro-perovskites having general formula ABF_3, is an important category of halide perovskites.[11,12] The unique physical properties of fluoro-perovskites[13–15] have made them functional in various scientific disciplines like geophysics, astrophysics, electrical ceramics, optical oscillators, and particle accelerators.[16–19] Although part of theoretical and experimental studies (lattice constant, bulk modulus, tolerance factor) of alkali-based fluoro-perovskites, $RbYbF_3$ and $CsYbF_3$, have been reported, complete investigations are still required.[20–25]

To utilize the waste heat from running vehicles and factories, materials with acceptable thermoelectric (TE) properties have attracted the attention of scientific community in recent years[26] Conversion of waste heat into electrical power can be made possible by devices made of high thermal efficiency materials.[27,28] The efficiency of thermal device is calculated from the figure of merit:[29] $ZT = \sigma TS^2/\kappa$. For obtaining large thermoelectric efficiency, electrical conductivity (σ), Seebeck coefficient (S), and thermal conductivity (κ), the materials with $ZT \geq 1$ can be used in thermoelectric devices, however, improvement in ZT value is a tricky task for the researchers because S, σ, and κ are strongly independent of each other. Moreover, improvement of power factor and demotion of lattice conductivity are two major challenges in the improvement of ZT value of a TE material.[28] At present, materials with high ZT values are fewer, however efforts are in progress to enhance ZT in more materials like $PbTiO_3$, $BaTiO_3$, $SrTiO_3$, $Bi2Te_3$, and $CoSb_3$.[30–32] Nano TE mate-

*Two of the authors, Asif Mahmood and S M Ramay, were supported by the Deanship of Scientific Research at King Saud University (Grant No. RGP-311).
†Corresponding author. E-mail: qmmustafa@iau.edu.sa
‡Corresponding author. E-mail: ahayat@ksu.edu.sa
© 2020 Chinese Physical Society and IOP Publishing Ltd

rials (Al-ZnO/RGO,[33] $BaTiO_3$/RGO[34]) obtained by mixing oxides with reduced graphene oxide (RGO) are demanded on a large scale due to their high ZT values. By exhibiting high ZT, these nancomposites have proved their dominance over individual materials. Investigators of material science are still searching for high ZT materials with excellent thermoelectric performances. The Wiedemann–Franz law describing the interdependence of κ_e (carrier thermal conductivity) and σ (electrical conductivity) reveals that high σ and small κ values are pre-requisite to get high ZT.

2. Calculation method

The FP-LAPW + lo method based on Wien2k code[35] was utilized in order to analyze the behavior of the studied perovskites. We analyzed the $RbYbF_3$ and $CsYbF_3$ perovskites in cubic phase through volume optimization process and determined the ground state parameters by using Murnaghan equation of states.[36] The volume optimization of studied perovskites was carried out by using PBEsol approximation.[37–39]

The Becke and Johnson (mBJ) potential was modified to increase the band gap of studied materials.[40] The mBJ potential was used to adjust the lattice constant for the exact bandgap that caused the electronic states to be improved. The default value (-6 Ry, 1 Ry $= 13.6056923(12)$ eV) of cut-off energy was used for implementing all calculations. In addition, the Gaussian factor (G_{max}) and angular momentum vector (l_{max}) are kept at 18 and 10 respectively. The selection of k-mesh was considered to be the most important element in order to acquire the accuracy of these calculations. We plotted energy *versus* k-points graph after testing several k-meshes. For the present computations, we chose the critical value of k-mesh ($10 \times 10 \times 10$) at which the energy becomes constant. Chapin's method[35] was used in order to calculate the elastic constants. Similarly, for the cubic symmetry, tensor matrix was solved by the Chapin's method. Consequently, BoltzTraP code[41] was taken into account for elaborating the thermoelectric properties that depend on the temperature and chemical potential.

3. Results and discussion

3.1. Structure stability and electronic behavior

The structures of $RbYbF_3$ and $CsYbF_3$ with space group (221)-$Pm3m$ are optimized by PBEsol to reduce the lattice strain. The optimized electronic structure and optimized curves are displayed in Figs. 1 and 2. The calculated values of lattice constant a, bulk moduli B, enthalpy of formation ΔH, and band gap of fluoride-based perovskite $RbYbF_3$ and $CsYbF_3$ are listed in Table 1.

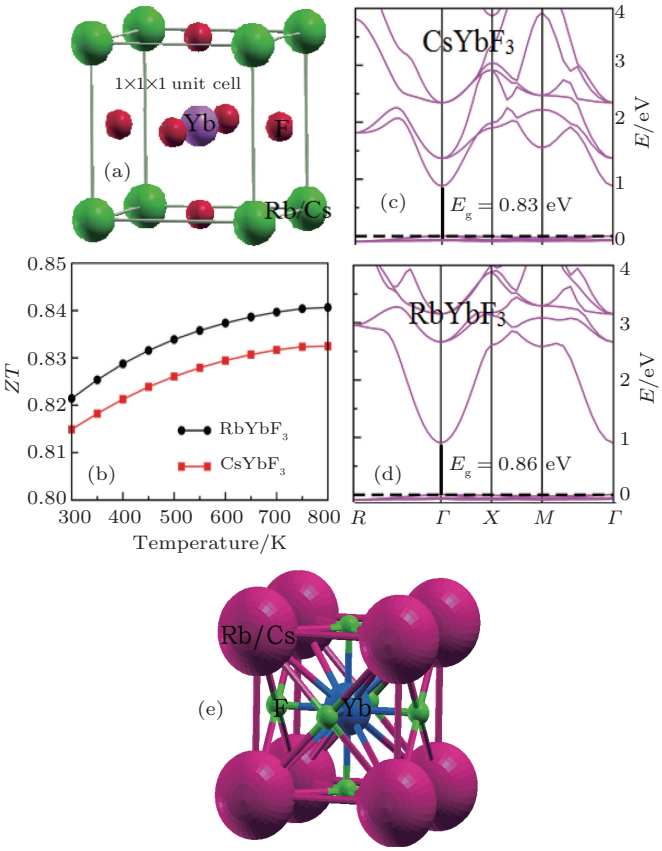


Fig. 1. (a) Electronic structures, (b) energy band structure, figures of merit of (c) $CsYbF_3$, (d) $RbYbF_3$, and (e) calculated crystal structure of Rb/$CsYbF_3$ formed by Xcrysden.

Table 1. The calculated values of lattice constant a, bulk moduli B, enthalpy of formation ΔH, and band gap of fluoride-based perovskites $RbYbF_3$ and $CsYbF_3$.

Parameter	$RbYbF_3$	$CsYbF_3$
a_0/Å	4.60, 4.53[a]	4.67, 4.61[a]
B_0/GPa	41.86	37.62
ΔH/(eV/unit cell)	−2.50	−2.26
Band gap $E_g(\Gamma$–$\Gamma)$/eV	0.86	0.83

[a]Ref. [24].

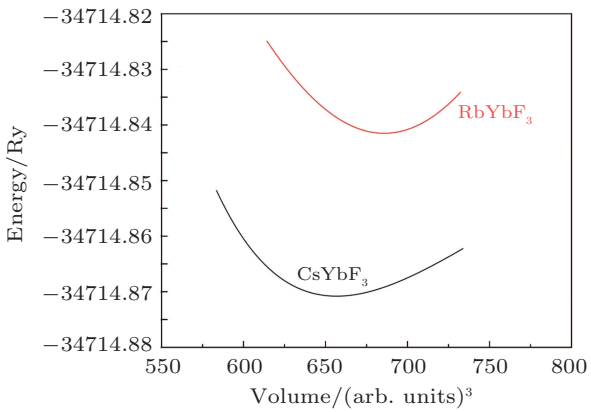


Fig. 2. Plot of optimized energy *verses* volume of $CsYbF_3$ (red) and $RbYbF_3$ (black) calculated by PBEsol approximation.

The Rb/Cs atoms are located at the corners of cube, and Yb atoms are occupied by the tetrahedron of F atoms. The calculated lattice constants $a = 4.60$ Å and $a = 4.67$ Å for $RbYbF_3$ and $CsYbF_3$ are consistent with the results in Refs. [42,43]. The lattice constant of $CsYbF_3$ is larger than that of $RbYbF_3$ because of larger atomic radius of Cs than that of Rb. The bulk modulus B (in unit GPa) decreases from 41.86 GPa (Rb) to 37.62 GPa (Cs) because the increasing of atomic size reduces the binding forces between electrons and nucleus. The structural and thermodynamic stability of the studied materials are determined by Goldsmith's tolerance factor (t_G) and formation energy (ΔH). The tolerance factor is given by $t = (r_{Rb/Cs} + r_F)/\sqrt{2}(r_{Yb} + r_F)$, where $r_{Rb/Cs}$, r_{Yb}, and r_F are the radii of individual Rb/Cs, Yb, and F atoms, respectively.[44] The ideal value of t_G is one for cubic perovskites however, the range of t_G from 0.94 to 1.02 is also valid. The value of t_G is 0.94 for $RbYbF_3$ and 0.99 for $CsYbF_3$, which shows the studied compounds have stable structures. Furthermore, thermodynamic stability has been reported in Refs. [45,46] demonstrating that the negative value shows the energy releasing during compound formation and confirming the existence of thermodynamic stability. The band structures are plotted in Fig. 3, showing that the direct band gap is 0.86 eV in the Γ direction in the first BZ for $RbYbF_3$ and 0.83 eV for $CsYbF_3$.

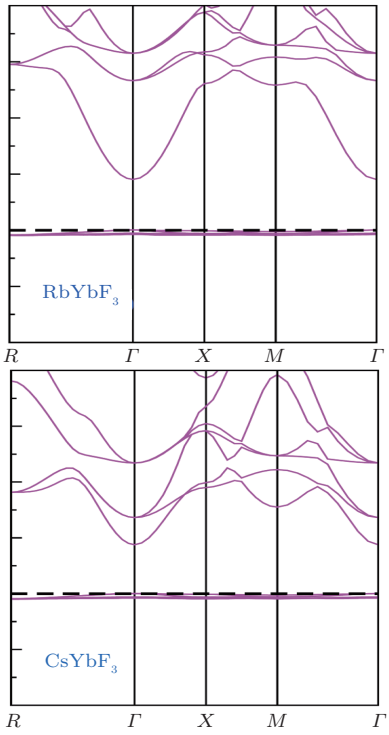


Fig. 3. Electronic band structures of (a) $RbYbF_3$ and (b) $CsYbF_3$ calculated by PBEsol+mBJ potential.

3.2. Thermoelectric properties

The transport properties of $RbYbF_3$ and $CsYbF_3$ are plotted in Figs. 4–8. The BoltzTraP code has been implemented to analyze them.[47,48] The expression for transport coefficient $\sigma_{\alpha\beta}(\varepsilon)$ of electrical conductivity is mathematically expressed as

$$\sigma_{\alpha\beta}(\varepsilon) = \frac{1}{N}\sum_{i,k}\sigma_{\alpha\beta}(i,k)\frac{\delta(\varepsilon-\varepsilon_{i,k})}{\delta(\varepsilon)}, \tag{1}$$

$$\sigma_{\alpha\beta}(i,k) = e^2\tau_{i,k}\upsilon_\alpha(i,\boldsymbol{k})\upsilon_\beta(i,\boldsymbol{k}), \tag{2}$$

where τ is the relaxation time, $\upsilon_\beta(i,k)$ is the group velocity, N is the number of k-points, and k is the wave vector representing the group velocity. To calculate the necessary parameters for analyzing the thermoelectric behavior, the integration of transport coefficient is conducted as follows:

$$\sigma_{\alpha\beta}(\alpha,\mu) = \frac{1}{\Omega}\int\sigma_{\alpha\beta}(\varepsilon)\left[-\frac{\partial f_0(T,\varepsilon,\mu)}{\partial\varepsilon}\right]\mathrm{d}\varepsilon, \tag{3}$$

$$S_{\alpha\beta}(T,\mu) = \frac{1}{eT\Omega\sigma_{\alpha\beta}(T,\mu)}\int\sigma_{\alpha\beta}(\varepsilon)(\varepsilon-\mu) \times\left[-\frac{\partial f_0(T,\varepsilon,\mu)}{\partial\varepsilon}\right]\mathrm{d}\varepsilon. \tag{4}$$

These equations are analyzed through BotzTraP code to check the thermoelectric properties. The calculated thermal conductivities (σ) versus μ (in unit eV) and T (in unit K) are presented in Figs. 4(a) and 4(b), with μ being the energy needed to add electrons by facing Coulomb potential. The positive value of μ represents n-type character and the negative value represents the p-type character.[49,50] The electrical conductivity from 1 eV to 3 eV is high which shows that the conduction electrons are available at high energy. The σ peak has large intensity for $CsYbF_3$ than that for $RbYbF_3$ because electrons are easily available for the conduction in $CsYbF_3$. The σ value decreases with temperature (800 K) increasing due to the insulating behavior of the material under study. Comparatively, the electrical conductivity of $CsYbF_3$ is higher than that of $RbYbF_3$ because of the reason as explained above.

The thermal conductivity (κ) is related to the flow of heat by electron movement (κ_{el}) and lattice vibration (κ_{ph}).[51] The lattice vibration produces an elastic wave of energy which moves along with electrons. In our calculations, the thermal conductivity of phonons is ignored because it is beyond the BoltzTraP code limits and only confers the electronic part of κ. The calculated values of κ are shown in Figs. 5(a) and 5(b). The thermal conductivity starts to increase when chemical potential is 1 eV for $RbYbF_3$ and it is 1.4 eV for $CsYbF_3$ and reaches to maximum intensity at 2.5 eV. Its value is large at 2.5 eV for $CsYbF_3$, which may be due to the interactions among a large number of electrons. The electrical conductivity decreases with the temperature increasing at a faster rate than electrical conductivity, which may be due to the insulating behavior of materials under investigation. Moreover, κ/σ is small (10^{-5}), which shows that the more electrons are available for conduction.[52,53]

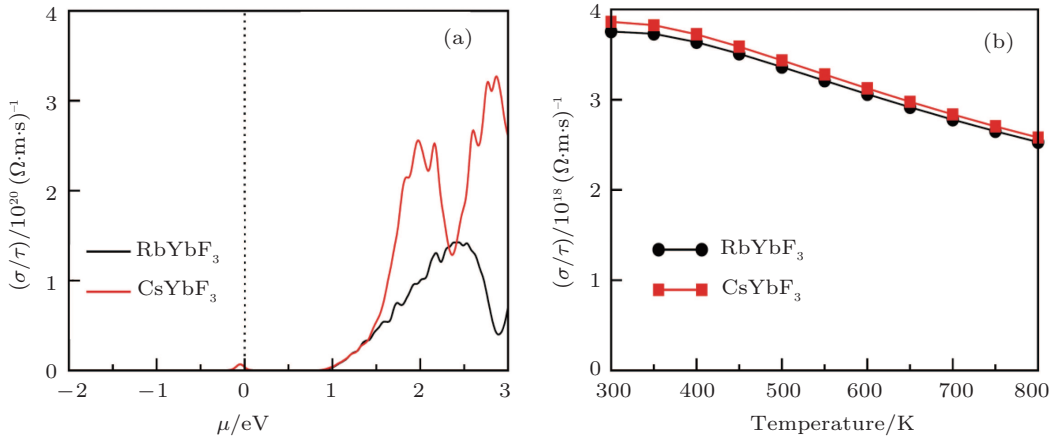


Fig. 4. Electrical conductivity of $RbYbF_3$ and $CsYbF_3$ against (a) chemical potential and (b) temperature.

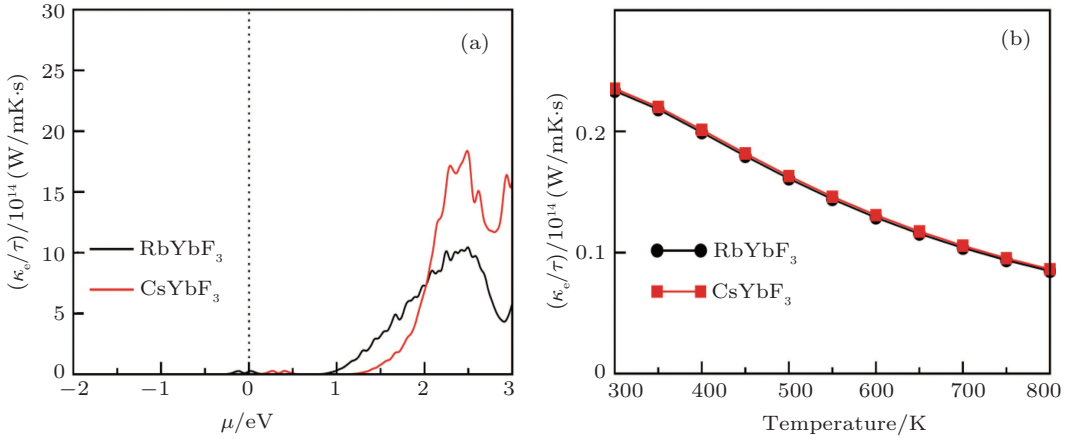


Fig. 5. Thermal conductivity of $RbYbF_3$ and $CsYbF_3$ against (a) chemical potential and (b) temperature.

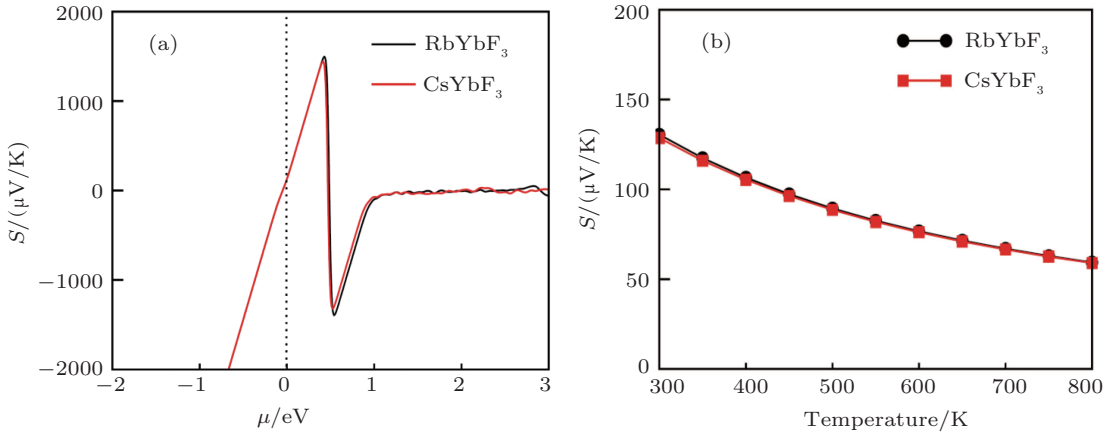


Fig. 6. Seebeck coefficient of $RbYbF_3$ and $CsYbF_3$ against (a) chemical potential and (b) temperature.

Seebeck coefficient (S) shows that the potential difference varies with temperature difference between contacts of two dissimilar metals. In semiconductors, both the electrons and holes contribute to Seebeck coefficient. The calculated Seebeck coefficient increases to 1200 μV/K and then drops to −1200 μV/K at 0.5 eV, which shows that the electrons and holes are present as carriers (see Fig. 6(a)). The effect of temperature on Seebeck coefficient is displayed in Fig. 6(b). It decreases with temperature increasing up to 800 K. The power factor ($S^2\sigma$) measures thermal efficiency without thermal effects. The power factor (PF) *versus* μ and T are shown in Figs. 7(a) and 7(b), respectively. The intensities of collective peaks around the Fermi level of $CsYbF_3$ cancel the effect due to opposite charge carriers while in an energy range from 0.8 eV to 3 eV the large number of peaks are detected, which shows that the conversion of thermal heat into electrical energy is triggered by the electrons. The power factor decreases with increasing T because both Seebeck coefficient and electrical conductivity decease. To measure it, the actual efficiency of the power factor of the material under study must be divided by thermal conductivity, which is explored by the figure of merit $ZT = (S^2\sigma/\kappa)T$, where T is the absolute tempera-

ture (see Figs. 8(a) and 8(b)).[53] Its value at Fermi energy and 0.5 eV are both zero and maxima are at 0.3 eV and 0.8 eV. The values of ZT are increases linearly with temperature. The ZT values of $RbYbF_3$ are higher than those of $CsYbF_3$ in the whole temperature range. For the easy understanding of transport properties, their values at 300 K are listed in Table 2. The ZT value of $RbYbF_3$ is 0.82 and that of $CsYbF_3$ is 0.80, which shows their applications in heat conversion devices.

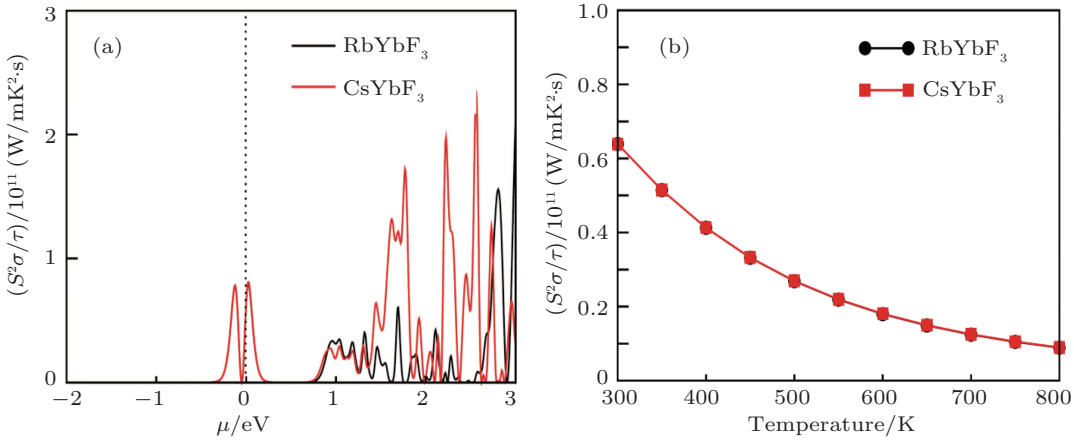


Fig. 7. Power factor of $RbYbF_3$ and $CsYbF_3$ against (a) chemical potential and (b) temperature.

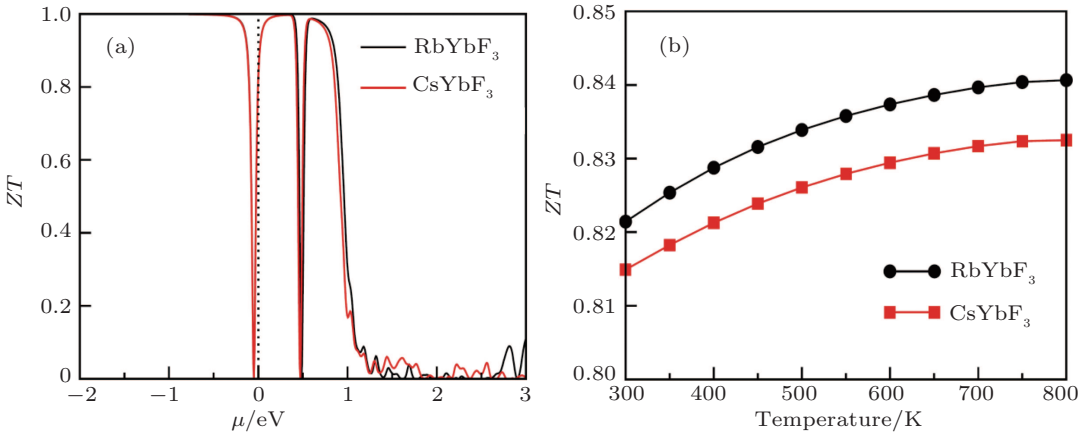


Fig. 8. Figure of merit (ZT) of $RbYbF_3$ and $CsYbF_3$ against (a) chemical potential and (b) temperature.

Table 2. Calculated room temperature values of electrical conductivity (σ), thermal conductivity (κ), Seebeck coefficient (S), power factor (σS^2), and figure of merit (ZT) for fluoride-based perovskites $RbYbF_3$ and $CsYbF_3$.

Perovskites	$\sigma/10^{18}$ $(\Omega\cdot m\cdot s)^{-1}$	$\kappa/10^{14}$ $(W/mK)^{-1}$	$S/(\mu V/K)$	$\sigma S^2/10^{12}$ $(W/mK^2\cdot s)$	ZT
$RbYbF_3$	3.76	0.230	130.44	0.639	0.82
$CsYbF_3$	3.86	0.235	128.60	0.638	0.81

4. Conclusions

We explored the electronic and transport properties of alkali metal-based halides. The $RbYbF_3$ and $CsYbF_3$ have thermodynamically stable cubic structures. The lattice constant and bulk modulus are consistent with the results in the existing literature. The small band gap of 0.86 eV for $RbYbF_3$ and 0.83 eV of $CsYbF_3$ are important for thermoelectric characteristics. The κ/σ is on the order of 10^{-5}, which confirms the materials under study to possess the thermoelectric applications. Moreover, the results show n-type character. The figure of merit for $RbYbF_3$ and $CsYbF_3$ at room temperature are 0.82 and 0.80, which increase with the augment of temperature. Therefore, the compounds under study have large potential applications in thermoelectric generators and refrigerators.

Acknowledgement

The authors (Asif Mahmood and Shahid M Ramay) extend their appreciation to the Deanship of Scientific Research at King Saud University for funding the work through the research group project No. RGP-311.

References

[1] Mathur N andwood P L 2003 *Phys. Today* **56** 25
[2] Moskvin S, Makhnev A A, Nomerovannaya L V, Loshkareva N N and Balbashov A M 2010 *Phys. Rev. B* **82** 035106

[3] Weeks C and Franz M 2010 *Phys. Rev. B* **82** 085310
[4] Murtaza G, Ahmad I, Amin B, Afaq A, Maqbool M, Maqssod J, Khan I and Zahid M 2011 *Opt. Mater.* **33** 553
[5] Kagan C R, Mitzi D B and Dimitrakopoulos C D 1999 *Science* **286** 945
[6] Klauk H 2000 *Phys. World* **13** 18
[7] Ramesh R and Spaklin N A 2007 *Nat. Mater.* **6** 21
[8] Scott J F 2006 *J. Phys.: Condens. Matter* **18** R361
[9] Bokov A A and Ye Z G 2006 *J. Mater. Sci.* **41** 31
[10] Dar S A, Srivastava V, Sakalle U K, Parey V and Pagare G 2017 *Mater. Res. Express* **4** 106104
[11] Huang K, Feng M, Goodenough J and Milliken C 1997 *J. Electrochem. Soc.* **144** 3620
[12] Rao K and Yoon K 2003 *J. Mater. Sci.* **383** 91
[13] Murtaza G and Ahmad I 2011 *Physica B* **406** 3222
[14] Murtaza G, Ahmad I, Maqbool M, Rahnamaye-Aliabad H A and Afaq A 2011 *Chin. Phys. Lett.* **281** 17803
[15] Ghebouli B, Ghebouli M A, Fatmi M and Bouhemodou A 2010 *Solid State Commun.* **150** 1896
[16] Erum N and Iqbal M A 2017 *Chin. Phys. B* **26** 047102
[17] Heaton R A, Harrison J G and Lin C C 1983 *Phys. Rev. B* **28** 5992
[18] Erickson E M, Ghanty C and Aurbach D 2014 *J. Phys. Chem. Lett.* **5** 3313
[19] Bai Y, Yu H, Zhu Z, Jiang K, Zhang T, Zhao N, Yang S and Yan H 2015 *J. Mater. Chem. A* **3** 9098
[20] Moreira R L and Dias A 2007 *Phys. Chem. Solids* **681** 617
[21] Wu G Q and Hoppe R 1983 *Z. Anorp. Allg. Chemie* **504** 55
[22] Verma A S and Kumar A 2012 *J. Alloys Compd.* **541** 210
[23] Jiang L Q, Guo J K, Liu H B, Zhu M, Zhou X, Wu P and Li C H 2006 *Phys. Chem. Solids* **67** 1531
[24] Verma A S and Jindal V K 2009 *J. Alloys Compd.* **485** 514
[25] Ubic R 2007 *J. Am. Ceram. Soc.* **90** 3326
[26] Li J F, Liu WS, Zhao L D and Zhou M 2010 *NPG Asia Mater.* **2** 152
[27] Zhao L D, Berardan D, Pei Y L, Byl C, Pinsard-Gaudart L and Dragoe N 2010 *Appl. Phys. Lett.* **97** 092118
[28] Dehkordi A M, Zebarjadi M, He J and Tritt T M 2015 *Mater. Sci. Eng. R Rep.* **97** 1
[29] Goldsmid H J 2010 *Introduction to Thermoelectricity* (Berlin, Heidelberg: Springer-Verlag)
[30] Rahman G and Rahman A U 2017 *Physica B* **526** 122
[31] Amin B, Singh N, Tritt T M, Alshareef H N and Schwingenschlögl U 2013 *Appl. Phys. Lett.* **103** 031907
[32] Li H, Tang X, Zhang Q and Uher C 2009 *Appl. Phys. Lett.* **94** 10114
[33] Nam W H, Kim B B, Seo S G, Lim Y S, Kim J Y, Seo W S, Choi W K, Park H H and Lee J Y 2014 *Nano Lett.* **14** 5104
[34] Mallada C, Menendez J L, Dura O J, de la Torre M A R, Menendez R and Santamaria R 2017 *J. Eur. Ceram. Soc.* **37** 3741
[35] Blaha P, Schwarz K, Madsen G K, Kvasnicka D and Luitz J 2001 Wien2k An augmented plane wave+ local orbitals program for calculating crystal properties
[36] Murnaghan F D 1944 *Proc. Natl. Acad. Sci. USA* **30** 244
[37] Blaha P, Schwarz K, Sorantin P and Trickey S K 1990 *Comput. Phys. Commun.* **59** 339
[38] Wu Z and Cohen R E 2006 *Phys. Rev. B* **73** 235116
[39] Becke A D 1988 *Phys. Rev. A* **38** 3098
[40] Tran F and Blaha P 2009 *Phys. Rev. Lett.* **102** 226401
[41] Madsen G K and Singh D J 2006 *Comput. Phys. Commun.* **175** 67
[42] Ullah R, Ali M A, Murad S, Khan A, Dar S A, Mahmood I and Laref A 2019 *Mater. Res. Express* **6** 125901
[43] Hautier G, Fischer C, Ehrlacher V, Jain A and Ceder G 2019 *Inorganic Chemistry* **17** 656
[44] Young J and Rondinelli 2016 *J. Phys. Chem. Lett.* **7** 918
[45] Mahmood Q, Hassan M and Noor N A 2016 *J. Phys.: Condens. Matter* **28** 506001
[46] Sabir B, Murtaza G, Mahmood Q, Ahmad R and Bhamu K C 2017 *Current Appl. Phys.* **17** 1539
[47] Madsen G K H, Schwarz K and Singh D J 2006 *Comput. Phys. Commun.* **175** 67
[48] Scheidemantel T J, Ambrosch-Draxl C, Thonhauser T, Badding J V and Sofo J O 2003 *Phys. Rev. B* **68** 125210
[49] Bilal M, Saifullah, Shafiq M, Khan B, Aliabad H A R, Asadabadi S J, Ahmed R and Ahmad I 2015 *Phys. Lett. A* **379** 206
[50] Hassan M, Shahid A and Mahmood Q 2018 *Solid State Commun.* **270** 92
[51] Mahmood Q, Hassan M, Ahmed S H A, Shahid A and Laref A 2018 *J. Phys. Chem. Solid* **20** 87
[52] Yasukawa M, Kono T, Ueda K, Yanagi H, Kim S W and Hosono H 2013 *Solid State Commun.* **172** 49
[53] Hassan M, Mahmood Q and Ramay S M 2019 *Mater. Res. Express* **6** 126110